TSF031

The Simulation of Flow Field inside the Wankel Combustion Chamber

Thanapol Poojitganont, Husni Taher Izweik, Heinz Peter Berg

Brandenburg University of Technology Cottbus, Univ.-Prof. Dr.-Ing. H.P. Berg,
Chair of combustion engines and flight propulsion, Cottbus 03046, Germany
Tel: +49 355 69 4850, E-mail: poojitth@tu-cottbus.de

Abstract

This research is the first step for the complete rotating simulation of the Wankel combustion engine. The stationary volume at zero degree of crank angel is used for calculate the air flow in three different shapes of geometry models. The FIRE program is used as a simulation tool. And the input pressures are also varied to investigate the change of velocity field inside the volume.

The results from this research show the flow characteristics which are caused by different pressure input and also different shapes of geometry. It seems that the variation of the input pressure does not make too much effect on the velocity profile. The result from this simulation will be utilized for validation with experimental results. Moreover, the ensuing knowledge can also be applied for design the suitable chamber geometry which will be achieved the optimal situation of mixture formation in the Wankel engine.

Keywords: rotary engine, Wankel engine, mixture formation, combustion chamber.

1. Introduction

The Wankel engine (Figure 1) belongs to the group of combustion engines with internal combustion. It is the engine which is more attractive power to weight ratio than the normal reciprocating engine. It also has small number of parts. In addition to, it moves rotational during its operation thus the Wankel engine is more balanced and smoothness [1].

Figure 1. The Wankel engine on an engine test-bed

The rotary engine can be treated and evaluated with respect to performance characteristics as a displacement type internal combustion engine of four-stoke, one-cycle similar to the reciprocating engine [2]. And for any combustion engines, to reach the maximum power output, the mixture formation inside the engine should be considered [3].

The spray characteristic from the injector and the geometry of the combustion chamber are two main parameters which are involved in mixture formation mechanism. This research has concentrated firstly on the effect from the geometry of its combustion chamber. The different shapes of the chamber can provide unlike fluid flow characteristics and the understanding of these phenomena can be used for optimization the suitable situation of mixing between air flow and fuel droplet inside the combustion chamber.

Eventually, the results from this research will be compared with the experimental stationary model's results at the same degree of crank angle. And both of them will be used for validate the complete rotating simulation of the Wankel engine. In addition to, the understanding of the flow phenomenon and also the mixture formation can be utilized for designing the combustion chamber of Wankel engine as well.
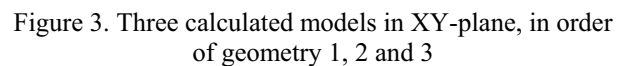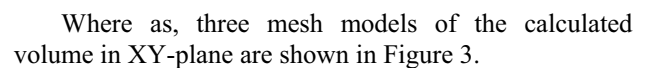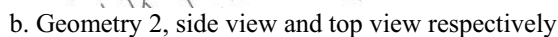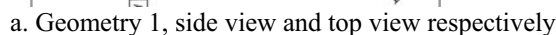
2. Nomenclature

The scientific symbols which are used in this work have been explained in this section.

2.1. Latin symbols

C_μ	constant in turbulence model
$C_{\varepsilon 1}$, $C_{\varepsilon 2}$, $C_{\varepsilon 3}$, $C_{\varepsilon 4}$	
	constants in the modeled ε equation
G	body force production
k	turbulent kinetic energy
P	mean-strain production
P_i	input static pressure
P_o	output static pressure
S_{ij}	rate of strain
t	time
U_i	velocity in i-direction
v	velocity component in y-direction
w	velocity component in z-direction

School of Mechanical Engineering , Suranaree University of Technology

2.2. Greek symbols

Π_i	dimensionless input pressure
ε	rate of turbulent energy dissipation
μ	dynamic viscosity
μ_t	dynamic turbulent viscosity
ν_t	eddy viscosity
ρ	density
σ_k	turbulence Prandtl number for variable k
σ_ε	turbulence Prandtl number for variable ε
σ_ρ	turbulence Prandtl number for variable ρ

3. Simulation setup

The simulation tool in this research is the program which is called FIRE. It is the Computational Fluid Dynamics (CFD) software which uses the finite volume method to simulate fluid flow [4]. Moreover, this program can also be used to simulate spray injection and engine combustion as well.

3.1. Geometry and mesh modeling

With in this research, as it has already been mentioned, the three geometries have been calculated with four different pressure input. The calculated models at zero degree of crank angle have been used. The combustion chamber shapes created from the drawings of the rotary engine rotors as shown in Figure 2 which have been provided by Wankel Super-Tec GmbH, Germany.

a. Geometry 1, side view and top view respectively

b. Geometry 2, side view and top view respectively

c. Geometry 3, side view and top view respectively

Figure 2. Side view and top view drawings of the different rotor geometries

Where as, three mesh models of the calculated volume in XY-plane are shown in Figure 3.

Figure 3. Three calculated models in XY-plane, in order of geometry 1, 2 and 3

3.2. Boundary condition

The dimensionless parameter (Π_i) between the input pressure and the output pressure has been created in this study. It can be defined as Equation (1).

$$\Pi_i \ = \ \frac{P_i}{P_o} \tag{1}$$

The dimensionless input pressure has been varied from 2.5, 5.0, 7.5 and 10.0. The output region has been setup as the atmospheric pressure. The inner side surface along the longitudinal of the volume has been set as symmetry because this simulation has calculated only a half of the real geometry volume. The rest surfaces have been defined as wall. The illustration of boundary setup on geometry 1, for instant, is shown in Figure 4.
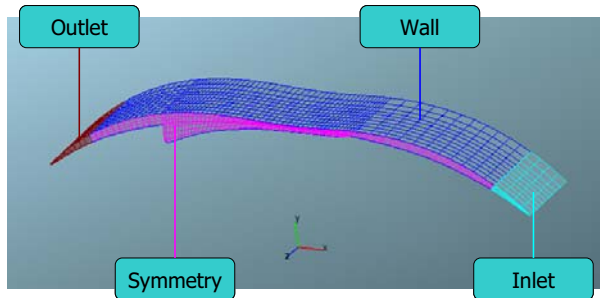
School of Mechanical Engineering , Suranaree University of Technology

Figure 4. The boundary setup on geometry 1.

3.3. Calculation parameters

The important calculation parameters are shown in Table 1.

Table 1. Calculation parameters

Parameters	Geometry 1	Geometry 2	Geometry 3
Total cells	8447	15046	6411
Volume, m^3	1.828×10^{-5}	1.984×10^{-5}	2.121×10^{-5}
Run mode	Time step	Time step	Time step
End time, s	0.003	0.003	0.003
Fluid	Air	Air	Air
Equations	Momentum, Continuity, Energy	Momentum, Continuity, Energy	Momentum, Continuity, Energy
Turbulence model	$k - \varepsilon$	$k - \varepsilon$	$k - \varepsilon$
Scheme	Central differencing, Upwind	Central differencing, Upwind	Central differencing, Upwind

The $k - \varepsilon$ model which has been used in this simulation can be defined as [5, 6]

$$\rho \frac{\partial k}{\partial t} + \rho U_j \frac{\partial k}{\partial x_j} = P + G - \varepsilon + \frac{\partial}{\partial x_i}\left(\mu + \frac{\mu_t}{\sigma_k}\frac{\partial k}{\partial x_j}\right)$$
(2)

$$\rho \frac{D\varepsilon}{Dt}$$

$$= \left(C_{\varepsilon 1}P + C_{\varepsilon 3}G + C_{\varepsilon 4}k\frac{\partial U_k}{\partial x_k} - C_{\varepsilon 2}\varepsilon\right)\frac{\varepsilon}{k} + \frac{\partial}{\partial x_j}\left(\frac{\mu_t}{\sigma_\varepsilon}\frac{\partial \varepsilon}{\partial x_j}\right)$$

where

$$P = 2\nu_t S_{ij}S_{ij} - \frac{2}{3}\left(\mu_t S_{kk} + k\right)S_{kk} \qquad (3)$$

$$G = -\frac{\mu_t}{\rho\sigma_\rho}\nabla\rho \qquad (4)$$

$$\mu_t = C_\mu \rho \frac{k^2}{\varepsilon} \qquad (5)$$

And the coefficients have the standard values according to Table 2.

Table 2. Standard values of coefficients

C_μ	$C_{\varepsilon 1}$	$C_{\varepsilon 2}$	$C_{\varepsilon 3}$	$C_{\varepsilon 4}$	σ_k	σ_ε	σ_ρ
0.09	1.44	1.92	0.80	0.33	1.00	1.30	0.90

4. Results and discussion

The results are illustrated in the cut-section of the calculated volume both in XY-plane and in YZ-plane. The coordinate and positions of the cut-section can be defined as Figure 5.
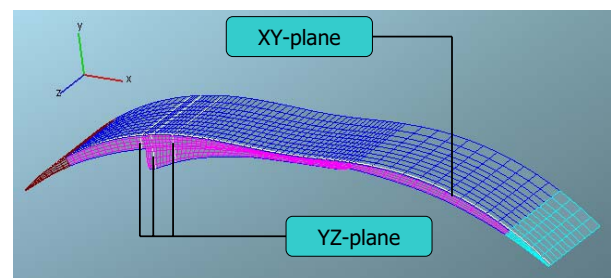

Figure 5. Cut positions of the calculated volume

4.1. Development of calculated velocity in time

As mention above, this research has used time step mode for calculation. The development of velocity in time steps of geometry 1, in case $\Pi_i = 10.0$ has been illustrated in Figure 6.
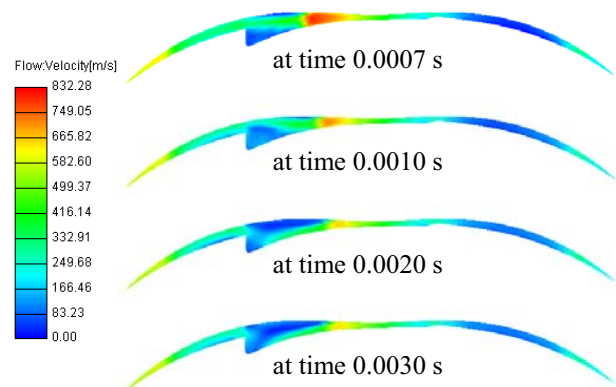

Figure 6. XY-plane velocity results in four time steps

The results show that the effect of input pressure has been distributed along the calculated volume after time step 0.002 second because there is no significant different of velocity field between time step 0.002 second and 0.003 second. This can be claimed that in this case of study the velocity in the simulated volume tend to be steady after calculation time 0.002 second.

School of Mechanical Engineering , Suranaree University of Technology

4.2. Different input pressure

In a case of different input pressure, the velocity results of geometry 2 at time step 0.003 second are shown in Figure 7, Figure 8 and Figure 9 in XY-plane, YZ-plane at position x = -0.040 meter and x = -0.048 meter from center of the calculated volume respectively.
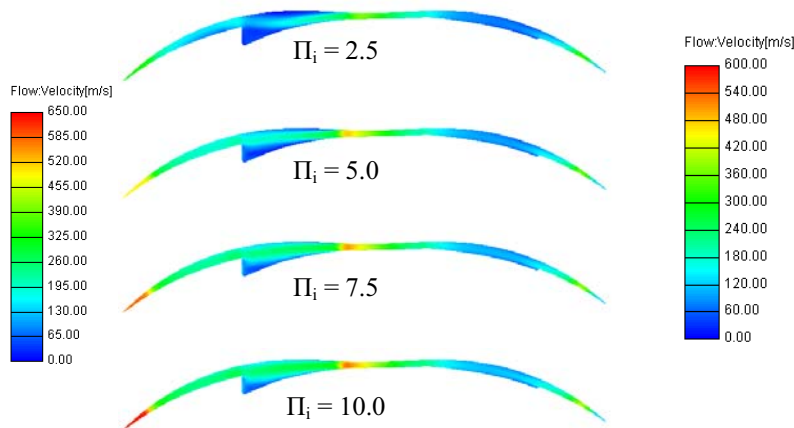

Figure 7. XY-plane velocity results in different pressures

From the results, they have shown that the different input pressure did not make too much effect both on the flow field along the calculated volume and also on the flow field across the volume. In Figure 7, there is only small expansion of high velocity region above the end of combustion chamber position when the input pressure has been increased.
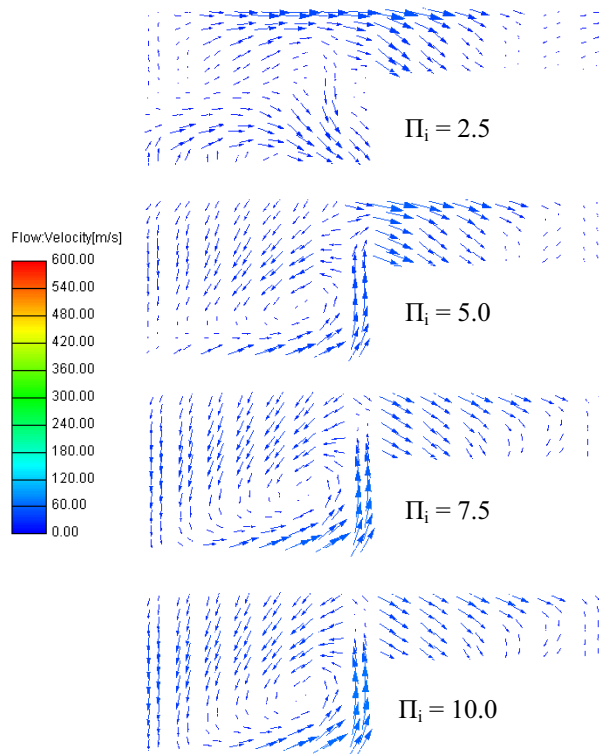
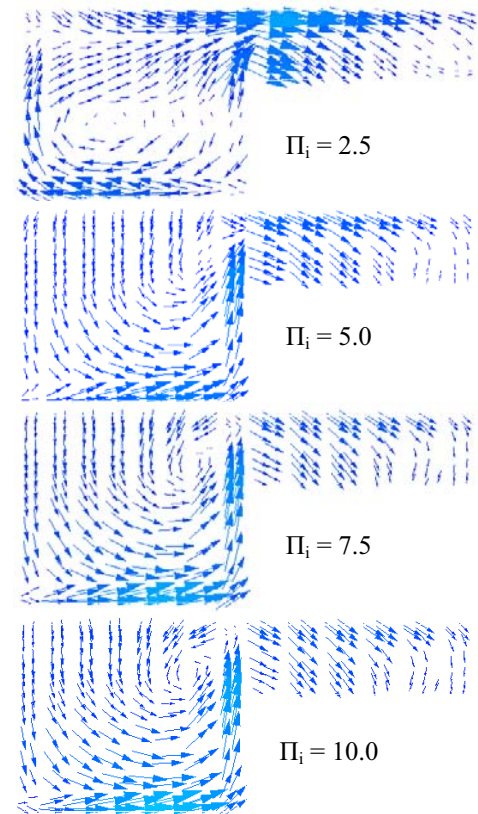Figure 8. YZ-plane velocity results, at position x = -0.040 m from center of simulated volume

Figure 9. YZ-plane velocity results, at position x = -0.048 m from center of simulated volume

In cross-section results (Figure 8 and Figure 9), there are circulation flows inside the calculated volume, these flows are caused from immediately changed of the combustion chamber geometry. These phenomena will be useful for the mixture formation process between air flow and fuel droplet in the operating engine.

The difference in magnitude of cross-section velocities of the two low dimensionless input pressures ($\Pi_i = 2.5$ and $\Pi_i = 5.0$) has occurred but it seems that the magnitude of velocities which are governed by the two high dimensionless input pressure do not change when they are compared together. This can be claimed that the limit boundary of input pressure for this kind of calculation is approximately at $\Pi_i = 7.5$.

4.3. Difference model geometry

The compared results on the different volume geometries at time step 0.003 second with input pressure $\Pi_i = 2.5$ and $\Pi_i = 7.5$ in XY-plane are shown in Figure 10 and Figure 11 respectively.
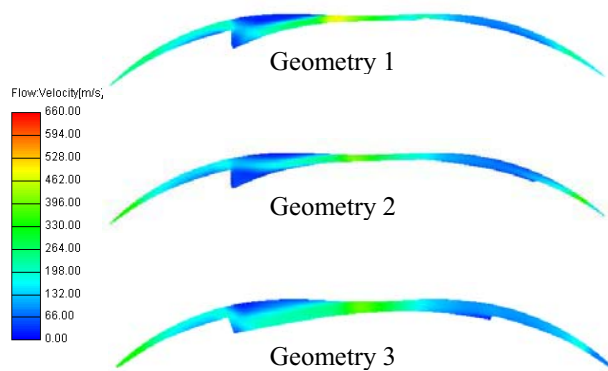
School of Mechanical Engineering , Suranaree University of Technology

TSF031

Figure 10. XY-plane velocity results, Π_i = 2.5

For low input pressure range (Π_i = 2.5) as shown in Figure 10, the flow field inside the calculated volume of the geometry 1 has similar sub-region with the flow field from the geometry 2. But the magnitude of the first one is higher. In case of the third geometry, the flow field is different from the formers. There are three nearly zero sub-regions in the combustion chamber. And the maximum velocity region has occurred at the center of the calculated volume.
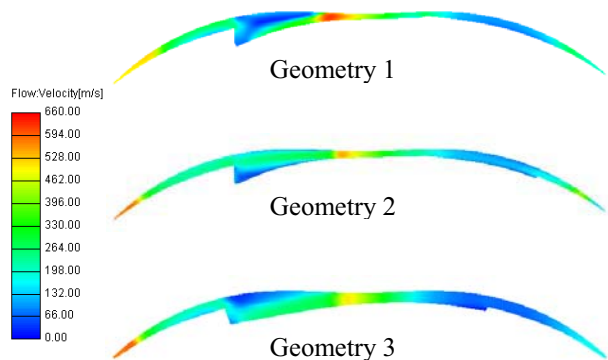

Figure 11. XY-plane velocity results, Π_i = 7.5

For high input pressure range (Π_i = 7.5) in Figure 11, there is similar character between the flow field from geometry 1 and geometry 2 at the upstream of the flow. Actually in mesh modeling there is a small difference between these two geometries. The geometry 2 has been added small volume at the upstream part of the first geometry.

In case of the third geometry, the flow field has similarly occurred as it was in the case of low input pressure.

The results in YZ-plane are shown in Figure12 with Π_i = 2.5 and in Figure 13 with Π_i = 7.5. Both of them show the projected velocity on YZ-plane ($v \cdot \overline{j}$ and $w \cdot \overline{k}$ velocity components) of geometry 1, 2 and 3 respectively.
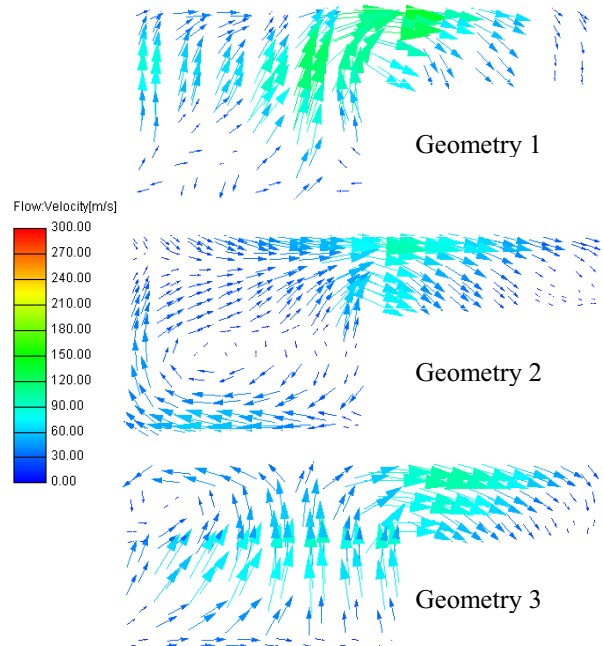

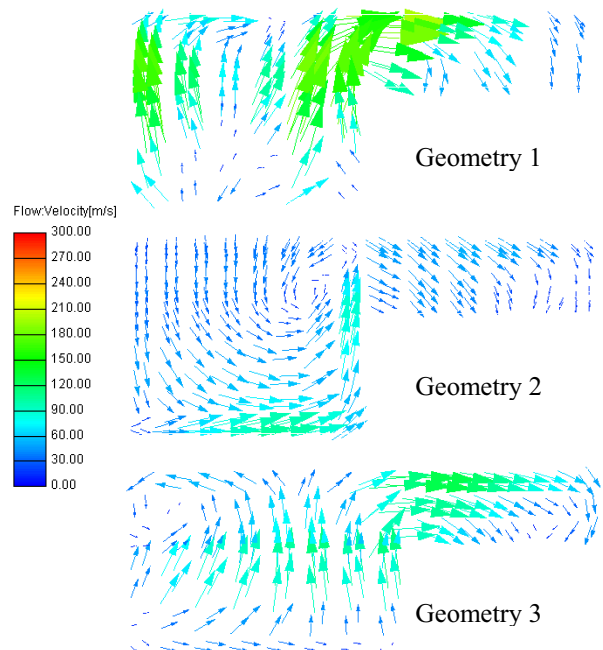
Figure 12. YZ-plane velocity results, Π_i = 2.5

Figure 13. YZ-plane velocity results, Π_i = 7.5

Only the results from the second geometries have shown the clear pattern of circulation velocity components but it is not clearly evident in the first and the third geometry.

5. Conclusion

In this case of simulation, the results in several different time steps indicate that the velocity along the calculated volume tend to be steady after calculation time 0.002 second.

TSF031

The similarly circulation flow characteristics have occurred perpendicular to the main flow in the simulated volume. These patterns will be very helpful in the mixture formation mechanism.

The different input pressure does not make too much effect on the velocity profile along the calculated volume and also on the velocity profile across the volume especially in the case of the dimensionless input pressure is higher than 7.5. But the input pressure takes petty effect on the velocity magnitude.

The compared results between the geometry 1 and the geometry 2 show that the increased volume at the upstream of the chamber does not send too much effect to the axial flow pattern, on the contrary, when the result from the geometry 3 has been compared, the added volume at the downstream of the chamber has governed the flow pattern particularly on the longitudinal plane of the calculated volume.

Acknowledgement

References
[1] Wankel Super-Tec GmbH, 2004. The New Generation of Wankel Rotary Engines. Cottbus, Germany.

[2] Yamamoto, K., 1981. Rotary Engine. Sankaido Co., Ltd., Tokyo, Japan.

[3] Stone, R., 1999. Introduction to Internal Combustion Engines. MACMILLAN PRESS, London, U.K.

[4] AVL LIST, 2000. User's Guide FIRE Version 7 and Swift Version 2. Graz, Austria.

[5] AVL LIST, 2004. CFD SOLVER v8.3. Graz, Austria.

[6] Davidson, L., 2003. An Introduction to Turbulence Models. http://www.tfd.chalmers.se/~lada (accessed on June 2006).